Experimental investigation of turbine wake flow by interferometrically triggered LDV-measurements

N. MAYRHOFER, H. LANG, J. WOISETSCHLÄGER

Institute for Thermal Turbomachinery and Machine Dynamics,

Graz University of Technology, Inffeldgasse 25, A-8010 Graz, Austria

EMail: ttm@ttm.tu-graz.ac.at Fax: +43 316 873 7234 Phone: +43 316 873 7227

ABSTRACT

Interferometrically detected density fluctuations had been used to trigger two-dimensional velocity measurements by Laser-Doppler-Velocimetry (LDV) in a turbine wake flow. The experiments were carried out in four circumferential lines behind a linear arrangement of turbine profiles with a chord length of 58mm at an isentropic exit Mach number of 0.69 and a Reynolds number of $9.75 \cdot 10^5$.

Density fluctuations of the vortex street were measured by guiding the beam of a laser-vibrometer through the turbine blade cascade behind the trailing edge under observation. The so derived time-signal was conditioned by means of an analog filter and used to synchronise the LDV system. Alternatively a more advantageous way using a phase-locked-loop (PLL) was applied. As result, phase resolved measurements of particle velocities in the wake of the profile could be derived. After decomposition into turbulent and periodic fluctuation the data were visualised and prepared for comparison to numerical results.

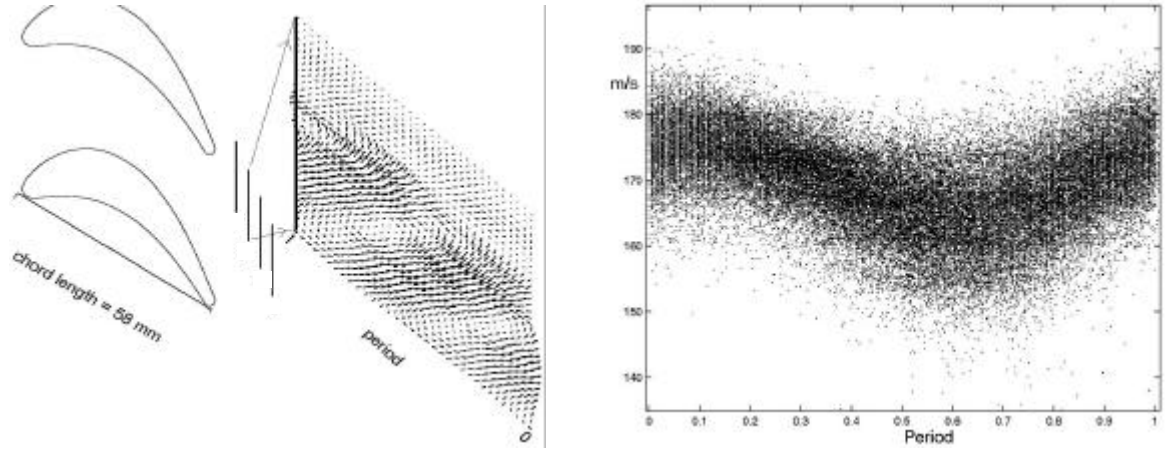

Fig. 1. Positions of the four planes for which time-resolved LDV measurements had been recorded in relation to the turbine blade profiles(left). For one plane the ensemble-averaged periodic changes of the velocity vectors are shown (middle). The time axis is plotted approximately against the direction of mean flow to show the vortices. For one position at the suction side a full LDV data set for one velocity component is presented at the right (18.3 kHz average vortex shedding frequency or 54.6 ms period). From these data time-averaged velocities as well as periodic, turbulent and total RMS were derived.

1. INTRODUCTION

The wake flow behind turbine blades together with the unsteadiness caused by the interaction between stator and rotor blades in turbomachines has significant impact on their efficiency and performance by affecting pressure distribution, boundary layer development and heat transfer for example. Filling of these wakes is an instationary process and can have high periodic components by formation of vortex streets especially in the subsonic regime (Cicatelli and Sieverding 1995). This periodic shedding of vortices can be excitation to mechanical systems such as bladings as well as a direct source of noise.

As numerical prediction of such effects forces the use of unsteady codes, the desire for comparison of the time-consuming results to detailed measurements is given (Sondak and Dorney 1999, Currie and Carscallen 1998).

Various studies have been carried out to determine different aspects of the shedding, as its frequency respectively Strouhal number (e.g. Sieverding and Heinemann 1990), influence on pressure distribution (e.g. Cicatelli and Sieverding 1997), energy distribution (Carscallen et al. 1999) or flow field (e.g. Zunino et al. 1997).

The experimental set-up described in this article is a phase-locked LDV measurement in the near wake of a linear turbine cascade. The changes in refractive index in the wake due to vortex shedding were detected by means of a laser-vibrometer and used as reference signal for synchronisation of the LDV system.

Before this phase resolved approach, a statistical decomposition of velocity histograms for the same flow conditions was performed and compared to unsteady Navier-Stokes code results (Gehrer et al. 2000).

2. EXPERIMENTAL SETUP

2.1. Test Facility

The tests were performed in a linear arrangement of seven VKI-LS59 turbine profiles (Kiock et al. 1986) installed into the transonic TTM wind tunnel of 100x230 mm flow cross section. Air was continuously supplied by a centrifugal-compressor, part of the compressor station by Atlas-Copco (Pirker et al. 1995).

An adjustable flat tailboard was used to optimise periodicity, controlled by pressure tappings on the test profile and its neighbours. Optical access to the flow was maintained by two flat glass windows of 100x180 mm size and 15 mm thickness. For cleaning, the cylindrical insert containing the profiles, windows and connections could be easily removed from the tunnel (Fig 2a).

The measurements were carried out at four circumferencial lines in the wake region of the test blade (Fig.2b). 20 positions were equally distributed over the indicated lines, point 1 at the suction side. Axial distances from the trailing edge were x/c = 0.083, 0.135, 0.187 and 0.238.

Table 1a: Cascade Geometry

Chord lenght c	58 mm
Aspect ratio h/c	1.72
Pitch to chord g/c	0.71
Trailing edge ratio d/c	0.05
Stagger angle βs	33.3°
arccos (t/c)	67.8°
Number of blades N	7

Table 1b: Test Conditions

Inlet angle β_1	30°
Exit Mach number M_{2is}	0.69
Reynolds Number Re_c	$9.75 \cdot 10^5$
Turbulence level Tu	5%
Total temperature T_{1tot}	308 K

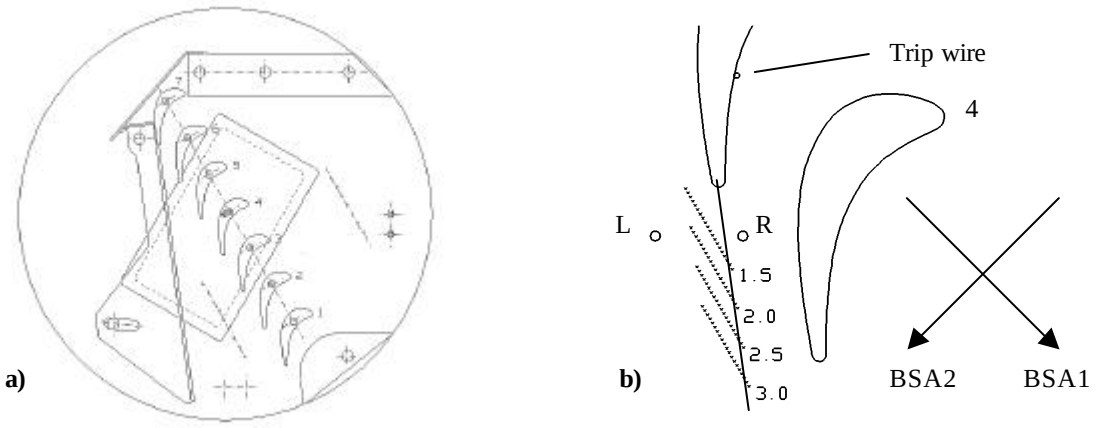

Fig. 2a) Cascade insert with blades, windows and tailboard. b) Detail of measurement planes in the wake region: Points L and R define the path of the vibrometer beam through the flow, arrows show LDV orientation, A line from the trailing edge centre under an angle of arccos (t/c) against the axial direction meets points 19.

2.2. Instrumentation

The standard instrumentation for the wind tunnel consists of an acquisition system including a 16-channel pressure-scanner ZOC14/16Px-50psid from Scanivalve and an amplifier for 7 thermocouples. These are used for aquisition of total and static pressures and total temperatures. Mach and Reynolds numbers are continuously calculated and displayed to control the compressor station.

The optical measurement was based on a two-dimensional LDV-system (Dantec Fiber-Flow) fed by an argon-ion laser from Coherent. Probe volume sizes were about 100 µm in diameter and 1.5 mm in length at fringe spacings of approximately 4 µm for the wavelengths 488 and 514.5 nm. Reflexes of the laser beams on the lens were masked out with pieces of adhesive tape. Positioning of the probe was done with Dantecs Lightweight traverse. Tracer particles were brought into the main flow smoothly by a probe of 6 mm diameter where the outflow velocity was close to that of the main flow with about 8 m/s before the nozzle. For control, acquisition and online visualisation of the collected data BSA Flow Software 1.2 was used.

Additionally a Polytec OVD 353 mid range laser-vibrometer provided basic information on the fluctuation of density in the wake. This laser-vibrometer, principally a Mach-Zehnder interferometer, is a standard tool for vibration analysis giving a high bandwidth signal of the integral optical phase change $\Delta\Phi$ along the line of propagation. z_0 and z_1 are the limits of the beam outside the device, n_0 the refractive index distribution at t = 0.

$$\Delta\Phi(x,y,t) = \frac{4p}{l}\int_{z_0}^{z_1}\left[n(x,y,z,t) - n_0(x,y,z)\right]dz$$

Due to this integral nature, all temporal fluctuations of the refractive index n in the laser-beam contribute to the signal derived as output (Mayrhofer and Woisetschläger 2000). For vibration measurement the upper integration limit z_1 is a function of time while n would be constant (Lewin et al. 1990). The refractive index n and density ρ stand in close relation, which can be assumed linear. The position of the vibrometer was chosen to cross the wake near the measuring planes of the LDV. An inclination of about 10 degrees against the trailing edge of the profile was introduced to reduce the influence of vortex structures located out of mid-plane, however it was also helpful to protect the vibrometer from the laser beams of the LDV. The beam of the vibrometer was transformed into a nearly parallel shape by means of a dispersing lens of 40 mm focus placed about 150 mm in front of the aperture and was finally reflected by a piece of retro-reflective foil after a length of approximately 340 mm.

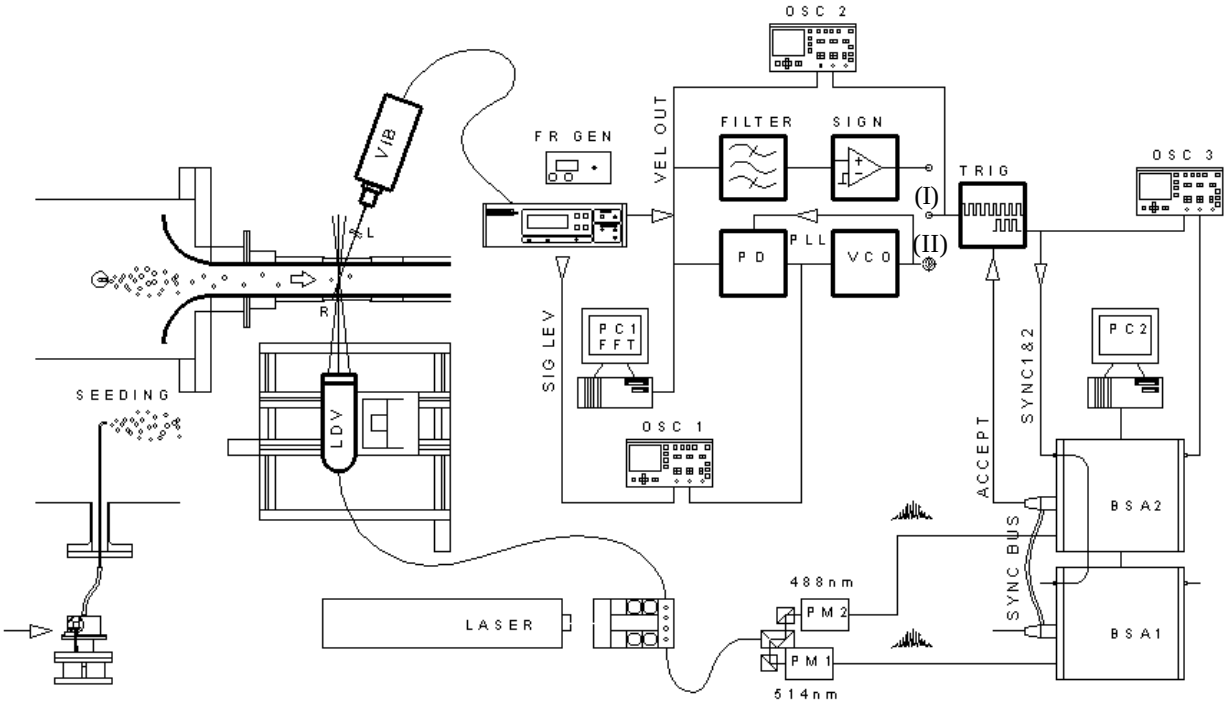

Fig. 3. Setup for time resolved wake-flow measurements. L: Lens, R: Retro-reflective foil, VIB: Vibrometer head, VEL OUT: Velocity output of vibrometer, SIG LEV: Signal level, PD: Phase detector, VCO: Voltage controlled oscillator, PM1&2: Photo-multipliers 1&2, TRIG: Trigger release unit, FR GEN: Frequency generator, SIGN: sign detector, OSC1,2&3: oscilloscopes 1,2&3, BSA1&2: burst spectrum analysers 1&2

For Spectral analysis of the vibrometer signal we used a NI4551 dynamic signal analyser card, allowing two channels of online Fast Fourier-Transform (FFT) up to a bandwidth of 95 kHz at 950 lines or continuous recording of two time signals. Programming of the system was done under LabVIEW from National Instruments. To prepare the vibrometer signal for synchronising the measurement, some conditioning was necessary. In a first step this contained an analog band-pass filter (Maxim MAX 274), followed by a sign detector (I). Later, a phase-locked-loop (Philips HCT7046A) turned out to be more suitable for our demand (II). Oscilloscope 1 was used for control of the level of VCO input, which gave information if the signal frequency stayed well within the lock-range without clipping or oscillating. The other channel was used to control the signal level of the vibrometer which is a logarithmic measure for the amplitude of the signal from the photo-detectors in this device. This level was kept at about 3V which is well above the maximum level of the display on the vibrometer itself. Oscilloscope 2 was operated in average mode and triggered by the synchronisation pulses. When there was correlation between vibrometer signal and sync pulses, the periodic content of the vibrometer signal could be seen changing more or less slowly depending on the chosen number of averages.

The synchronisation pulses were connected to the SYNC1 input of both BSA's, which stored and transferred their arrival times (AT) together with the valid particle data. Due to the high frequency of synchronisation pulses most of the SYNC pulses were not necessary for deriving the phase of particle transit in the vortex cycle.

For suppression of the unnecessary pulses a device was designed to release a defined number of synchronisation pulses after every detected Doppler burst. These events are indicated by the ACCEPT-outputs of the BSA's synchronisation-bus as described in the BSA manual (Dantec 1994). Access to these pins was provided by customised adapters. Oscilloscope 3 showed BSA bursts and synchronisation pulses.

2.3. Test Procedure

Search for appropriate flow conditions was done using the FFT signal of the vibrometer. For better understanding of the phenomena some experiments were carried out at varying flow conditions.

At a Re number of $7 \cdot 10^5$ an increase in turbulence occurred together with development of a clear signal peak at a Strouhal number of about 0.25 which was dominating up to Re $=1 \cdot 10^6$ where it was replaced by a different mode at almost the same frequency. Although intensive tests were done and obviously good spectra could be derived, a flow condition showing well-resolved LDV data could not be found. After application of a trip wire to the pressure side finally, these problems could be surpassed (diameter 0.1 mm, tape 0.05mm, 22 mm before TE). At a Mach number of 0.69 and a Reynolds number of $9.75 \cdot 10^5$ stable periodic flow conditions were reached.

For the filter application, after deriving the frequency of the vortex-street the band-pass was calculated and applied (centre frequency = 18200 Hz, pass-band width = 600 Hz @ -3dB, 8^{th} order Bessel).

Nevertheless this procedure had some disadvantages: Beside the time-consuming process of calculation and implementation of resistor values, at last by adjustment of precision trimmers, the filter had a high phase gradient $\partial\varphi/\partial f$ at small band-pass windows. The before mentioned phase-locked-loop was easier to adjust and had a much better phase response (Fig 4).

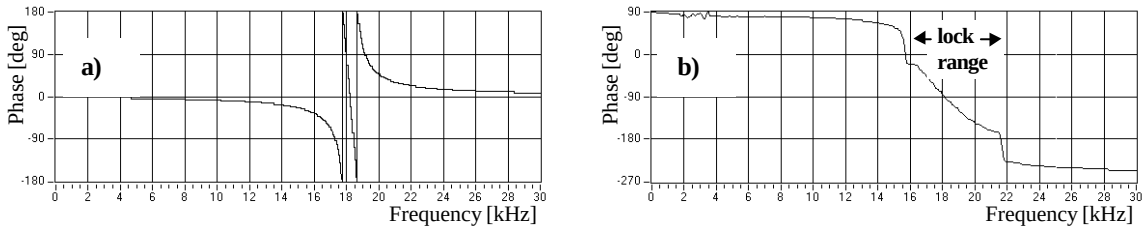

Fig. 4 Phase responses of filter (calculated) and PLL (measured). Phase gradients ¶j/¶f about 400 deg/kHz for the filter and 30 deg/kHz for the PLL. Fig b) is only a static characterisation of the PLL

The phase gradient of the filter depends on the chosen order and the selected band-pass width. Generally, the more selective the amplitude response has to be made, the worse the phase response becomes. Similar is valid for the PLL: The phase change over the lock-range is about constant, so a narrower lock range directly leads to a steeper phase response. When using the PLL we first adjusted its lock range by means of a frequency generator, the low-pass filter acting as controller between phase detector and voltage controlled oscillator (not shown in figure 3) was set relatively high so the output signal could follow the frequency changes of the vibrometer signal.

In the PLL circuit HCT7046 two phase detectors are available denoted as phase comparators in the product specification. We used phase comparator 1 which is an exclusive-or combination of input and VCO signal.

Now, so the change of phase (difference between SYNC-pulses and vibrometer signal) over frequency introduced a jitter to recorded arrival times and thus calculated phase positions, online display would only show modulation up to limited variation of the incoming frequency. Above this limits, totally smeared phase resolved velocity plots would have been a useless feedback to the user.

Initial tests were done with continuously running synchronisation to have online display of time resolved data.

After these our trigger-release was activated to shorten measurements and considerably reduce the amount of collected data. However this prevented online visualisation and made post-processing necessary, which was carried out in Matlab.

Table 2: LDV Parameters

Laser Parameters

Type:	Argon-Ion
Max Power:	7 W @ open Aperture
Power output used:	300 - 400 mW @ Aperture 6

Optics Parameters

Beam Separation:	38 mm
Beam Diameter:	2.2 mm
Focus nominal:	310 mm

Seeding Parameters

Generator:	Palas AGF 2.0D
Material:	DEHS (Diethylexylsebacat)
Density:	912 kg/m^3
Overpressure:	0.5 - 1 bar
Average Size:	0.3 µm after generator
Frequency $_{99\%}$:	95 kHz @ 0.3 µm calculated

Some General BSA Settings

High Voltage:	1104 V
Signal Gain:	36 dB
Pedestal Attenuation:	0 dB
Oversize:	OFF
Samples:	120000
Record Interval:	0.33 µs

Particle Statistics

Data Rate:	0,3 - 3 kHz
Validation:	40 - 20 %
Particles valid:	≈ 30000 per trav. pos.

2.4. Measurement Accuracy

Accuracy for the standard instrumentation was ±0.08% or ±2.8 mbar for the pressure scanner and ±1 °C for the temperature measurement.

The unknown distribution of particle diameters in the measuring volumes prevented a profound calculation of particle response in the oscillating fluid. It must be assumed that massive coagulation may have happened especially in the boundary layer of the profile. Calculation of frequency$_{99\%}$ for table 2 above was carried out following Ikeda et al. (1992). A more detailed analysis of velocity fidelity of particles in fluids is found at Mei (1996). Processing accuracy of the FFT can be assumed below 1%.

The phase error of one recorded particle mainly consists of the error due to the discretisation of possible arrival times (AT) and the variation of phase lag in the filter or PLL over frequency. The increment of possible arrival times is equal to the so called “record interval” for this processors which was 0.33 µs in our case, and thus also the maximum error for calculation of time differences. In values of calculated particle phase from two succeeding synchronisation pulses at an average period of 54.6 µs this gives 0.61 % of full cycle or 2.2 degrees. In terms of calculated frequency this is an increment of $\Delta f = 112$ Hz at 18300 Hz shedding frequency.

The second contribution to the phase error is due to the phase responses of filter or PLL. Although the actual period to every recorded particle was known, compensation of the phase lag can only be carried out down to an error of $\Delta\varphi = \partial\varphi/\partial f \cdot \Delta f$ which is about 54 deg for the applicated filter and 3.4 deg for the PLL alternative. Surely the strongest argument for use of the PLL in future measurements.

A further, difficult to handle source of error are possible uncorrelated particles due to instabilities in development of the vortex street which cause a smearing of particle phases over the whole cycle.

Relative changes of probe positions are neglected, estimated accuracy of traverse positions is 0.1 mm.

The airflow through the seeding generator was not measured, its input pressure was adjusted by means of a pressure regulator including relatively high uncertainty about the effective overpressure.

3. RESULTS AND DISCUSSION

The following results were derived by using the band-pass filter exclusively.

The vibrometer spectrum shown in Figure 5 was taken for the setup described in chapter instrumentation above and shows a clear peak for the periodic fluctuation in the wake while its second order is relatively small.

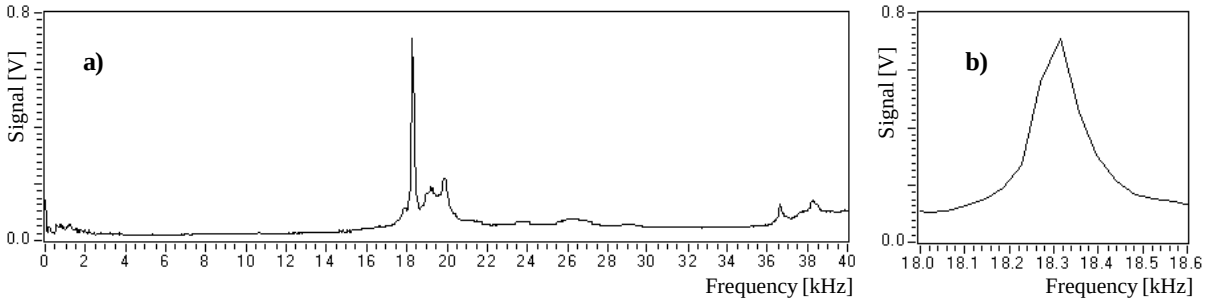

Fig. 5a). Amplitude Spectrum of Vibrometer signal (25 mm/sV, bandwidth 100 kHz). The peak at 18.3 kHz responds to an overall density fluctuation of 6.67×10^{-3} kg/m^3 across the cascade at a Strouhal number of St_d= 0.227. Vibrations of the test stand are visible below 4 kHz. Fig. b) shows a zoomed detail of the signal peak.

The smaller peak at 20 kHz (Std = 0.247) was likely to come from the neighbour profiles, as comparison with spectra for untripped profiles and the given Reynolds-number showed. The relation of peak amplitudes, especially the higher orders showed to change significantly with beam position.

The following figure shows examples of phase resolved data for the described measurement derived from calculation of the particle phase in relation to two synchronisation pulses released directly on the arrival of the particle. The data are not compensated for variation of filter phase.

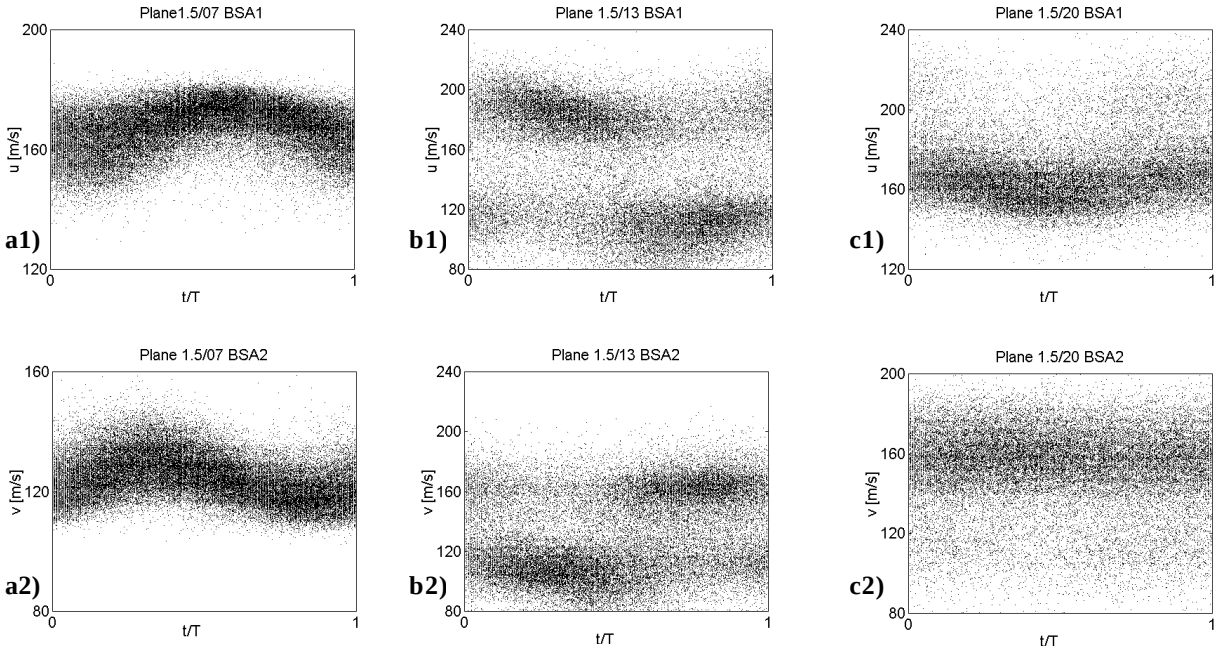

Fig. 6. Phase resolved velocity plots of measured particles for positions at the suction side (a1, a2), centre (b1, b2) and pressure side (c1, c2) of the wake in plane 1.5. T is the actual period at particle transit.

Remarkable is the fact that in the centre of the wake there was only small concentration of measured particles between the extreme values which might point on a problem with particle size in this region.

Velocity distribution in most phase sections was clearly non-gaussian.

Decomposition of velocity values u and v was done by the triple decomposition $u = \overline{u} + u_{per} + u'$ according to Reynolds and Hussain 1972, where $\overline{u}$ denotes the long-time average, $u_{per} = (\widetilde{u} - \overline{u})$ the periodic and u' the turbulent component of the instant velocity u . Values $\widetilde{u}$ were calculated as averages of u in 36 centred bins of 10 degrees width and $RMS_{turbulent}$ as the corresponding standard deviation. RMS_{total} is the standard deviation of u over $\overline{u}$ and $RMS_{periodic}$ of u_{per} over $\overline{u}$.

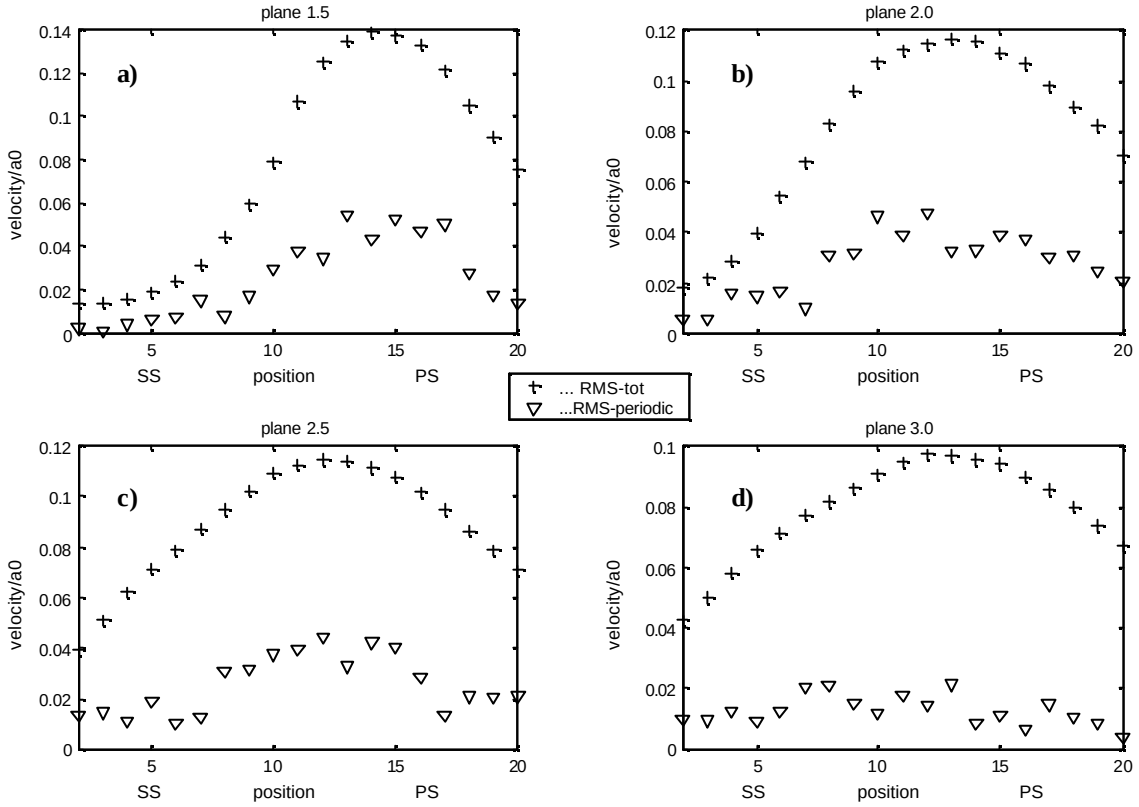

Fig. 7. Total and periodic RMS values of velocity in planes 1.5 to 3.0. Velocity values are referenced on a_0 the speed of sound at stagnation with 350 m/s.

RMS_{total} values showed smooth curves across the wake in every plane while the periodic values looked quite noisy. Varying signal stability leading to different amounts of uncorrelated measurements, as well as a variation in particle size either randomly over time or in direct consequence of the occurrences in the flow-field might be an explanation. Improved measurements in future will surely give answers to these speculations.

Picture 8 shows $RMS_{turbulent}$ values over the cycle. In plane 1.5 the distribution of turbulence across the phase clearly shows a wavelike behaviour in position as well as in intensity, compared to the pressure side the spatial gradient is higher at the suction side, separating the wake from the quite unaffected main-flow similar to the RMS_{total} in fig 7. These characteristics are gradually vanishing down to plane 3.0 where a more or less symmetrical and temporally constant $RMS_{turbulent}$ was observed.

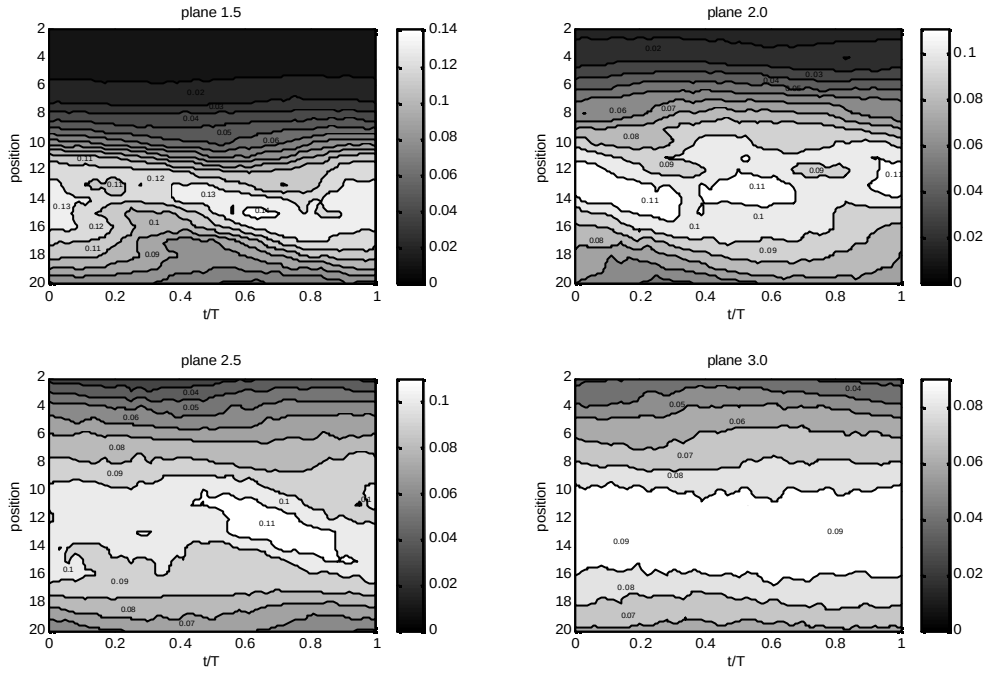

Fig. 8. Time-resolved $RMS_{turbulent}$ values of velocity in planes 1.5 to 3.0.

Due to the application of the described trip-wire results of planes 2.0 and 3.0 cannot be directly compared to those at Gehrer et al. (2000), where interpretations of velocity histograms are compared to results of different numerical codes. The main difference is that evaluation of the histograms gave high periodic and lower turbulent fluctuations being in agreement with the instationary calculations, while the actual phase-resolved results shown here have the opposite tendency, namely high turbulence values at relatively low periodic components. The evaluation of histograms worked on the hypothesis of two flow conditions sharing the whole shedding cycle according to the expected number of particles in two fitted normal distributions. This simplification is overestimating the periodic fluctuation for the cases of harmonic change of $\tilde{u}$.

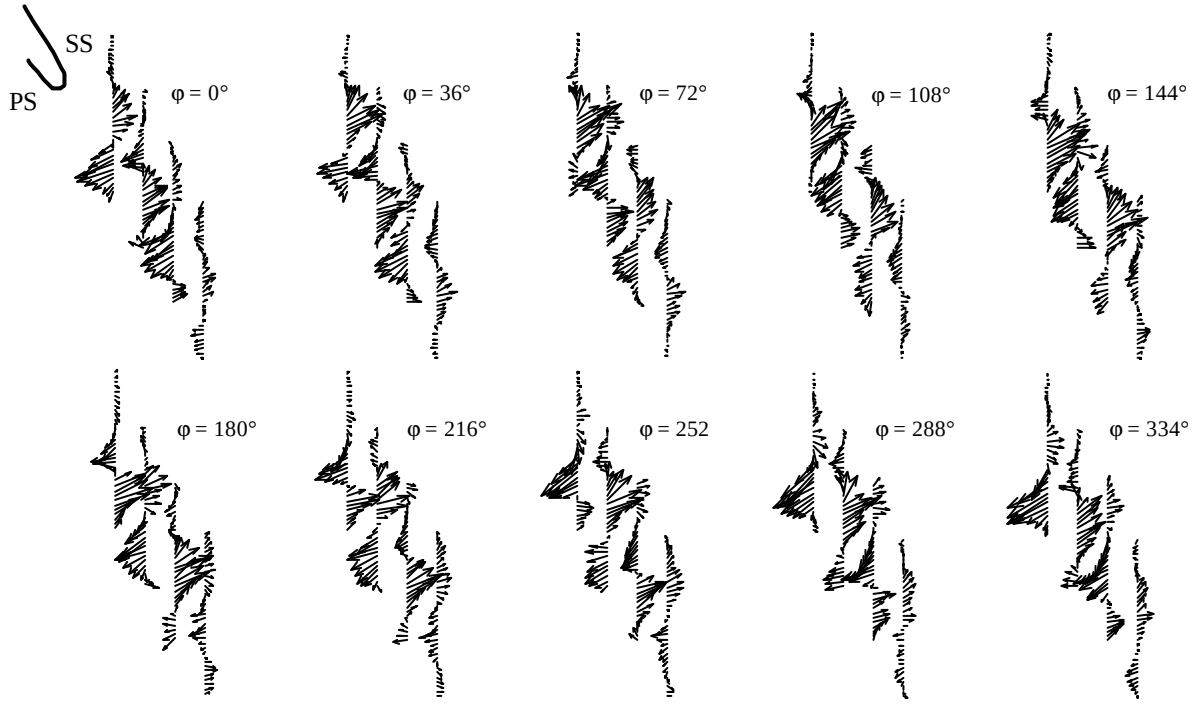

Fig. 9. Vector-field of velocities W_{per} in planes 1.5 to 3.0 (left to right) at discrete phases during shedding cycle

The periodic changes in the flow-field due to the passing of vortices is visible in figure 9. For example the fast decay of periodic intensity downstream, especially between plane 2.5 and 3.0. Detailed interpolation of streamlines into the vector field to determine the vortex positions was not carried out as the distance between planes is relatively big in relation to the vortex structures. The traverse increment used in the planes could be increased by a factor of two or three to uniformly cover a field of similar size in future measurements.

List of symbols

a	speed of sound	h	profile height	β	angle to axial direction
c	chord length	t	throat, time	φ	vortex phase
d	trailing edge diameter	u, v	velocity components	Φ	optical phase
f	frequency	W	velocity vector of u and v	u	kinematic viscosity
g	pitch				

$\mathrm{Re}_c = \frac{W_{2is} \cdot c}{u}$ Reynolds number $\quad St_d = \frac{f \cdot d}{W_{2is}}$ Strouhal number

4. SUMMARY

A non-invasive method for time-resolved velocity measurements with no need for calibration was applied to a turbine wake flow at a realistic shedding frequency of 18.3 kHz.

The velocity distribution within the vortex cycle could be resolved and visualised by ensemble averaging of instantaneous data.

Improvements are possible by checking of vortex stability and enabling or disabling measurement.

This checking might be done by comparing the signal amplitude after a filter to a threshold value or by the use of a lock-detector in a PLL.

As particle size is very critical, a study of seeding parameters by determination of particle size distribution in the wake should be of great evidence.

The rejection of oversized particles, which could not be used due to software problems should bring considerable improvement.

Earlier and more effective data reduction could shorten the time to result. As the actual software is not optimised for this kind of measurement we are currently working on a LabVIEW driver set for full control of the measurement.

One of the open questions is whether the success in tripping the boundary layer was due to separation of the test-profile's Strouhal number from those of its neighbours or whether the vortex street was not stable enough before that change. In the first case the same result should be achievable by tripping the neighbour-profiles only, which comes closer to the intention of non-intrusive measurement.

ACKNOWLEDGEMENTS

This work was supported by the Austrian Science Foundation (FWF) and the Austrian ministry for science and traffic and was part of the awarded grant Y57-TEC (Non-intrusive measurement of turbulence in turbomachinery). Thanks also to Dr. A. Gehrer for discussion of results and Dr. G. Siegmund from Polytec for providing closer details of the signal processing in the vibrometer.

REFERENCES

CARSCALLEN W. E., CURRIE T. C., HOGG S. I., GOSTELOW J. P. (1999): "Measurement and Computation of Energy Separation in the Vortical Wake Flow of a Turbine Nozzle Cascade" ASME Journal of Turbomachinery, Vol.121, pp.703-708

CICATELLI G., SIEVERDING C. H. (1995): "A Review of the Research on Unsteady Turbine Blade Wake Characteristics" AGARD PEP 85th Symposion on Loss Mechanisms and Unsteady Flows in Turbomachines, Derby, May 8-12, 1995

CICATELLI G., SIEVERDING C. H. (1997),: "The Effect of Vortex Shedding on the Unsteady Pressure Distribution Around the Trailing Edge of a Turbine Blade" ASME Journal of Turbomachinery, Vol.119 pp.810-819

CURRIE T. C., CARSCALLEN W. E. (1998): "Simulation of Trailing Edge Vortex Shedding in a Transonic Turbine Cascade" ASME Journal of Turbomachinery, Vol.120, pp.10-19

DANTEC (1994): "BSA enhanced Installation & User's guide" 9150A9307 Dantec Measurement Technology

GEHRER A., LANG H., MAYRHOFER N., WOISETSCHLÄGER J. (2000): "Numerical and Experimental Investigation of Trailing Edge Vortex Shedding Downstream of a Linear Turbine Cascade" ASME Turbo Expo 2000, Munich, Paper 2000-GT-0434

IKEDA Y., NISHIGAKI M., IPPOMMATSU M., HOSOKAWA S., NAKAJIMA T. (1992): "Optimum Seeding Particles for Successful LDV Measurements" S32-2, 6th International Symposion on Applications of Laser Techniques to Fluid Mechanics, Lisbon

KIOCK R., LEHTHAUS F., BAINES N. C., SIEVERDING C. H. (1986): "The Transonic Flow Through a Plane Turbine Cascade as Measured in Four European Wind Tunnels", ASME Journal of Engineering for Gas Turbines and Power, Vol. 108, pp. 277-284

LEWIN A., MOHR F., SELBACH H. (1990): "Heterodyn-Interferometer zur Vibrationsanalyse" Technisches Messen 57, Heft 9, 335-345

MAYRHOFER, N., WOISETSCHLÄGER J., 2000: "Frequency Analysis of Coherent Structures in Compressible Flows by Laser Vibrometry", in preparation for Experiments in Fluids

MEI R. (1996): "Velocity fidelity of flow tracer particles" Experiments in Fluids, Vol.22, pp.1-13

PALAS GmbH (1995): "Bedienungsanleitung Flüssigkeitszerstäuber AGF 2.0D" Palas GmbH, Karlsruhe, Jan. 1995

PIRKER H. P., JERICHA H., ZHUBER-OKROG G. (1995): "Auslegung und Betriebsverhalten einer Verdichteranlage für die Luftversorgung wissenschaftlicher Versuchseinrichtungen", VDI Berichte Nr.1208, pp. 331-347

REYNOLDS W.C., HUSSAIN A.K.M.F. (1972): "The mechanics of an organised wave in turbulent shear flow. Part 3. Theoretical models and comparisons with experiments", Journal of Fluid Mechanics, Vol. 54, Part 2, 1972, pp. 263-288

SIEVERDING C. H., HEINEMANN H. (1990): "The influence of Boundary Layer State on Vortex Shedding From Flat Plates and Turbine Cascades" ASME Journal of Turbomachinery, Vol. 112, pp.181-187

SONDAK D. L., DORNEY D. J. (1999),: "Vortex Shedding in a Turbine Cascade" Journal of Turbo and Jet Engines, Vol.16/2, pp.107-126

ZUNINO P., UBALDI M., CAMPORA U., GHIGLIONE A. (1997): "An Experimental Investigation of the Flow in the Trailing Edge Region of a Turbine Cascade" Proceedings of 2nd European Conference on Turbomachinery - Fluid dynamics and Thermodynamics, Antwerpen, pp.247-254